



## Experimental investigation on the formation and transport mechanism of outburst coal-gas flow: Implications for the role of gas desorption in the development stage of outburst



Kan Jin<sup>a,b,c,d</sup>, Yuanping Cheng<sup>a,c,d,\*</sup>, Ting Ren<sup>d,e,f,\*\*</sup>, Wei Zhao<sup>c,d</sup>, Qingyi Tu<sup>c,d</sup>, Jun Dong<sup>c,d</sup>, Zhenyang Wang<sup>c,d</sup>, Biao Hu<sup>c,d</sup>

<sup>a</sup> Key Laboratory of Coal Methane and Fire Control, Ministry of Education, China University of Mining and Technology, Xuzhou, Jiangsu 221116, China

<sup>b</sup> College of Quality & Safety Engineering, China Jiliang University, Hangzhou, Zhejiang 310018, China

<sup>c</sup> National Engineering Research Center for Coal and Gas Control, China University of Mining and Technology, Xuzhou, Jiangsu 221116, China

<sup>d</sup> School of Safety Engineering, China University of Mining and Technology, Xuzhou, Jiangsu 221116, China

<sup>e</sup> School of Civil, Mining & Environmental Engineering, University of Wollongong, NSW 2522, Australia

<sup>f</sup> State Key Laboratory of Coal Resources and Safe Mining, China University of Mining and Technology, Xuzhou, Jiangsu 221116, China

### ARTICLE INFO

#### Keywords:

Outburst

Coal-gas flow

Rapid gas desorption

Energy balance

### ABSTRACT

As the one of the most catastrophic hazards in underground mining, coal and gas outburst seriously threatens the safe mining of collieries. To understand the formation and transport mechanism of outburst coal-gas flow in roadway as well as evaluate the effects of gas desorption on its development, a new apparatus was developed to conduct simulated experiments with different gases of CO<sub>2</sub> and N<sub>2</sub>. Results indicated that the outburst coal-gas flow was a high-speed (up to 41.02 m/s during tests) gas-solid two phases flow with extreme complexity, its transport/destructiveness characteristics were significantly influenced by a number of factors including the outburst pressure, coal sample composition, ejection distance and so on. Among these factors, the gas desorption showed the greatest impact when compared to the controlled tests which only considered the effect of free gas expansion. With the effect of gas desorption, especially the rapid gas desorption from powdered coal, the total outburst energy could be promoted by 1.30–2.43 times; the peak values of outburst shockwave could be enhanced by at least 13.67%–63.22%; the transport type of coal-gas flow could be changed from dynamic pressure pneumatic conveying to the static pressure conveying which providing higher capability for outburst coal/rock conveying; the motion of ejected coal flow could have higher speed, longer transport duration and could suffer secondary acceleration. As the result, the destructiveness of outburst coal-gas flow would be remarkably intensified.

A further analysis for the energy consumption during the outburst coal-gas flow transport indicated that the free gas expansion energy was insufficient for the conveying of ejected coal (only accounting for less than half of the total energy), the difference of which was made up by the gas desorption, especially the rapid gas desorption from powdered coal (the average contribution ratio reached 56.0%, while the maximum reached 64.1%). Thus, it can be concluded that the rapid gas desorption from powdered coal played a decisive role on the promotion of outburst.

### 1. Introduction

Coal and gas outburst (hereinafter referred to as outburst) is an unstable release of the gas energy and strain energy that stored in a coal seam (An et al. 2013; Tu et al. 2016), accompanied by a sudden and violent ejection of large amounts of coal and gas from the working face into a limited working space in a short period (Chen 2011; Lama and

Bodziony 1998; Shepherd et al. 1981). Outburst is one of the most fatal dynamic disasters during underground mining, which can lead to serious damage to mineworkers' lives as well as underground mine infrastructures (Jiang et al. 2015; Wang et al. 2013b; Xu and Jiang 2017). Since the first documented outburst in France in 1834 (Flores 1998), > 40 thousand outburst accidents have been reported around the world (Fan et al. 2017), and almost half of which occurred in China

\* Correspondence to: Y. Cheng, National Engineering Research Center for Coal and Gas Control, China University of Mining and Technology, Xuzhou, Jiangsu 221116, China.

\*\* Correspondence to: T. Ren, School of Civil, Mining & Environmental Engineering, University of Wollongong, NSW 2522, Australia.

E-mail addresses: [ypc620924@gmail.com](mailto:ypc620924@gmail.com) (Y. Cheng), [tren@uow.edu.au](mailto:tren@uow.edu.au) (T. Ren).

(Jin et al. 2016b), which makes this country's coal mining industry the most outburst risk troubled sector in the world (Wang et al. 2013a; Ye et al. 2017a; Ye et al. 2018).

In the last 150 years, significant efforts have been made to fully understand the cause of outburst. And a number of theories/hypotheses were also proposed to explain the mechanism of outburst (Beamish and Crosdale 1998; Briggs 1921; Chen 2011; Karacan et al. 2011; Noack 1998), of which, theories such as dynamic theory (Farmer and Pooley 1967; Shepherd et al. 1981), combined-effects-driven theory (Hodot 1966; Zhao et al. 2017) and spherical shell destabilization theory (Jiang et al. 2015; Xu et al. 2006), are still of great guiding significance to nowadays research. Recently, as technology improves, the outburst mechanism was further studied. In their works, Peng et al. (2012) experimentally studied the influence of gas seepage on outburst, indicated that outburst can be treated as gas flow and deformation failure on fluid-solid coupling effect, and pointed out that the gas compression energy was the energy source for outburst as well as the source to throw and grind coal. Xue et al. (2011) considered the combining effects of stress-induced permeability changes, effective stress induced coal deformation and gas desorption-diffusion-flow in coal, proposed a coupled approach to numerically study the triggering of outburst. An et al. (2013), An and Cheng (2014) studied the effect of adsorbed gas on coal's deformation and mechanical properties, demonstrated the formation mechanism of low-permeability zones and its influence on the preparation and triggering of outburst. Tu et al. (2016, 2017) theoretically analyzed the failure process of outburst and indicated that the gas-enriched area in coal seam is an important reason to cause faster failure of coal. Zhi and Elsworth (2016) investigated the role of gas desorption on outburst by scaling analysis, indicated that the gas desorption induced by the elevated abutment stress was the main reason for triggering outburst. Zhao et al. (2016) studied the energy consumption during outburst and pointed out that rapid gas desorption from small-size coal particles within a short period was an essential condition for the development of outburst.

Even though abundant results have been achieved, due to the complexity of outburst there is still no single theory can explain the entire process of outburst (Fan et al. 2017; Xue et al. 2015). Moreover, according to the widely accepted method for outburst stages classification (see Fig. 1), it can be concluded that almost all of the theories mentioned above aimed at the preparation stage or trigger stage of the outburst. But field observations indicate that the destructiveness of outburst to the worker/facilities underground mainly comes from the transport of outburst coal-gas flow in underground roadway, which can result in the moving equipment, gas suffocation (Lu et al. 2014) and other secondary hazards like gas explosion (Lu et al. 2012; Ye et al. 2017b). However, the corresponding studies concerning the development stage of outburst or the transport process of outburst coal-gas flow are seriously lacking. Even if there exist some scholars who showed some interests on this issue, the research methods they took (can be generally divided into two categories as: 1. simplifying the outburst coal-gas flow as a uniformity jet flow and then study it with theoretical

or numerical analyses (Sun et al. 2011; Zhao et al. 2017); 2. treating the outburst as a physical explosion of high-pressure gas and then simplify the study of coal-gas flow transport as the propagation of shocked gas flow (Otuonye and Sheng 1994; Wang et al. 2012)) usually ignored the nature of such flow which showed significant characteristics of heterogeneous as well as extremely complex interphase interactions. Besides, due to the limitation of test conditions, previous studies could hardly provide any experimental data concerning the transport characteristics of outburst coal-gas flow.

Thus, to better understand the formation and transport mechanism of outburst coal-gas flow, in this article a new apparatus was used to give comprehensive investigations on the conveying/deposition characteristics of outburst coal-gas flow in underground roadway and the internal relations between outburst parameters (e.g. outburst pressure, sample property) and outburst's destructiveness (e.g. outburst intensity, shockwave overpressure, coal flow's motion speed). Additionally, the effect of gas desorption on the promotion of outburst coal-gas flow was also experimentally evaluated by using controlled tests. Conclusions from this work may help to reveal the outburst mechanisms as well as the transport characteristics of outburst coal-gas flow in underground roadway, which may also be able to provide some implications for the prevention of outburst disasters.

## 2. Sample and methods

### 2.1. Sample preparation

Coal samples used in the outburst coal-gas flow experiments were collected from the No. 10 coal seam of the Wolonghu Colliery, Anhui Province, China. Because almost all of the site outbursts were believed to have associations with the tectonically deformed coals (Aguado and Nieceza 2007; Kissell and Iannacchione 2014; Lama and Bodziony 1998; Lu et al. 2017; Paterson 1986; Xue et al. 2015) and the faster gas desorption from deformed coal which could promote the ejection of outburst coal (Jin et al. 2016a; Peng et al. 2012; Valliappan and Wohua 1999; Zhao et al. 2016). Thus, to give a comprehensive view on the outburst coal-gas flow transport, two different sized coal, namely the < 0.25 mm coal powder and the 1-3 mm coal particles, were prepared for the experiments. Of which, the < 0.25 mm coal powder was used to simulate the deformed coal induced by tectonic movement, while the 1–3 mm coal particle was used to simulate the destabilized and exfoliated normal coal in the outburst hole.

The basic parameters of the coal particle/powder were list in Table 1, and by mixing these two sized coals with various ratios, four kinds of experimental samples were prepared as shown in Table 2. The different initial gas desorption characteristics between these two sized coal are shown in Fig. 2, from which it can be noticed that the desorbed gas volume of < 0.25 mm coal powder in the first 5 s is 4.73 times higher than that of 1-3 mm coal particles, and this gap persists (although showing decrease trend) as time expands. With such a larger release of gas suddenly rushing into the roadway, the transport of

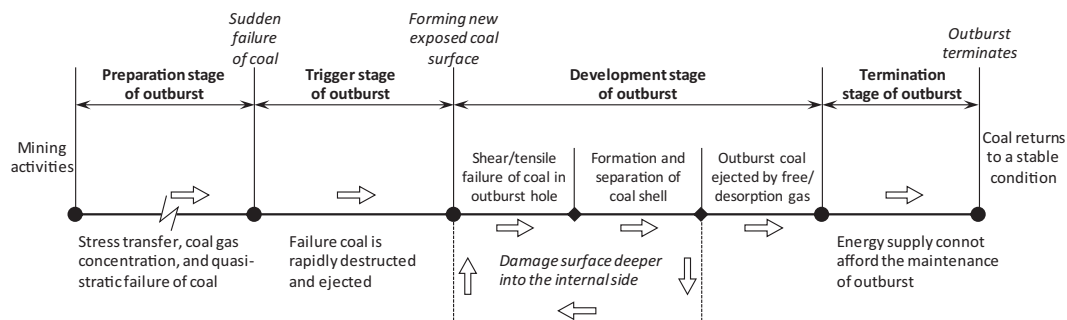


Fig. 1. Stage classification for the dynamic process of outburst.

**Table 1**  
Proximate analyses, porosities and methane ad-desorption parameters of the coal.

Particle size (mm)	Proximate analyses (wt%)				True density (t/m <sup>3</sup> )	Apparent density (t/m <sup>3</sup> )	Porosity (%)	Adsorption constant		$\Delta p$ (mm Hg)
	Mois	Ash	VM	FC				$V_L$ (m <sup>3</sup> /t)	$P_L$ (MPa)	
< 0.25	2.89	29.83	12.10	59.90	1.72	1.63	5.23	41.6522	0.7045	47.4
1–3	3.49	22.24	9.09	68.22	1.57	1.48	5.73	43.5640	0.5982	22.7

Mois = moisture; Ash is on a dry basis; VM = volatile matter, on dry ash free (daf) basis; FC = fixed carbon (daf basis);  $\Delta p$  = index of initial gas diffusion rate.

**Table 2**  
Preparation and ingredient of the experimental samples.

Sample ID	Percentage of different particle-sized coal (wt%)		True density (t/m <sup>3</sup> )
	< 0.25 mm coal powder	1–3 mm coal particle	
Sample #1	0	100	1.57
Sample #2	33.3	66.7	1.63
Sample #3	66.7	33.3	1.68
Sample #4	100	0	1.72

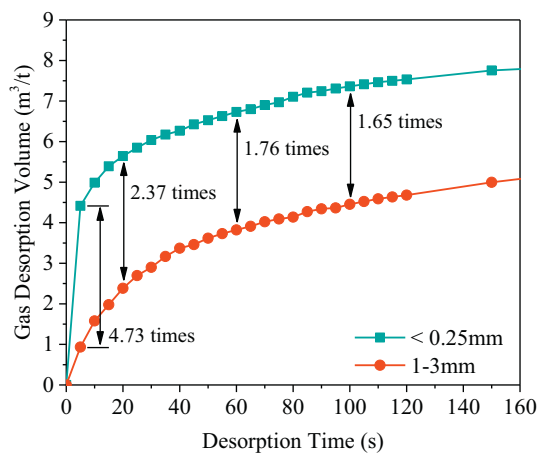


**Fig. 2.** Initial gas desorption characteristics of < 0.25 mm coal powder and 1–3 mm coal particles used in the experiments (equilibrium pressure: CO<sub>2</sub> 0.5 MPa).

outburst coal-gas flow would be definitely impacted with no doubt.

## 2.2. Experimental methods

### 2.2.1. Apparatus

To study the formation and transport of outburst coal-gas flow in underground roadway, a new apparatus was designed based on the theory of similarity. By using this new apparatus, features concerning the transport, deposition and destructiveness of outburst coal-gas flow (like the shockwave propagation, coal flow moving and ejected coal deposition) are able to be investigated.

The new apparatus is composed of five main parts, namely the outburst chamber (20 cm in diameter and 30 cm in length, can hold 8.6–11 kg of coal sample and withstand the gas pressure  $\leq$  5 MPa), decompression device (used to rapidly open the outburst chamber to trigger the ejection of outburst coal-gas flow), simulated roadway (assembled by five pipes made of high transmittance acrylic material, each pipe is 10 cm in diameter and 2 m in length), data acquisition system (composed of up to 2000 Hz high frequency pressure transmitters, high speed cameras, data acquisition card manufactured by National Instruments, USA and control software) and vacuum/gas injection equipment. Since the effect of geo-stress on outburst is mainly focused on crushing the coal mass prior to the triggering of outburst (Lu et al. 2014) whilst the ejection/transport of outburst coal mainly depend on

the gas energy (Peng et al. 2012; Valliappan and Wohua 1999), thus for the study of outburst coal-gas flow, the effect of geo-stress can be ignored and the tri-axial loading system is not needed for the experiment as well.

### 2.2.2. Experimental procedure

The critical procedure of experiment can be concluded as Fig. 3. After the loading of experimental sample, the airtight condition of the chamber is firstly tested by the helium gas. Then, according to different experimental purposes, various degassing and gas injection methods are applied. Since the field test data from Zhongliangshan Colliery indicated that the outburst coal-gas flow was not powered by the original gas pressure of the outburst-prone coal seam, but a static gas head of 0.3–0.6 MPa (Hu and Wen 2013; Zhao et al. 2016). Thus, in our tests, the experimental gas pressures were set to 0.1 MPa, 0.3 MPa and 0.5 MPa respectively. Once the equilibrium process is finished, the data acquisition system of apparatus will be connected and then the experiment will be triggered.

For safety's sake, CO<sub>2</sub> is used in the tests as the coal seam gas, instead of the explosive CH<sub>4</sub>. Moreover, N<sub>2</sub> is also applied to conduct controlled experiments (using Sample #1, Sample #2 and Sample #4) so that the effect of gas desorption on the outburst coal-gas flow can be experimentally evaluated. As one kind of weak adsorbent gases, the equilibrium adsorption capacity of N<sub>2</sub> for coal is only 13.5–29.2% of that for CO<sub>2</sub> under the same condition (Cui et al. 2004; Kelemen and Kwiatek 2009; Lin et al. 2018), and by further reducing the gas adsorption contact time between N<sub>2</sub> and coal (Zhao et al. 2014) it is reasonable to ignore the N<sub>2</sub> adsorption in the outburst chamber, which could provide a coal-gas flow driven only by the free gas in the chamber (without the participation of desorbed gas) as the comparison basis. The reason why chooses the N<sub>2</sub> gas but not the non-adsorbent helium gas to proceed the controlled tests is mainly attributed to helium's small density, which may fail to provide enough pneumatic conveying capacity for the transport of outburst coal-gas flow (the density of helium gas is only 9.05% of the CO<sub>2</sub> gas under the standard condition).

## 3. Results and analyses

### 3.1. Structure identification of outburst coal-gas flow

Combining the observations from experiments with some previous studies (Sun et al. 2009; Wang et al. 2012), the transporting state of outburst coal-gas flow in the roadway can be schematically described as Fig. 4. From the forefront of coal-gas flow to the undisturbed coal seam, successively there are shockwave front, area of compressed air, area of coal-gas flow and triggering area of the outburst.

Once outburst occurs, the high-pressure/speed coal-gas flow suddenly rushes into the roadway and expands, resulting in an intense compression of the air in the roadway as well as the continuously forming of a series of small compression waves in front of the compressed air. Because of the energy attenuation, the previously formed compression wave moves slower than the later formed one, and when the latter wave catches up with the former wave, an air shockwave will be produced (Wang et al. 2011). Usually, the shockwave propagates through the roadway with a supersonic speed and fatal overpressure, its

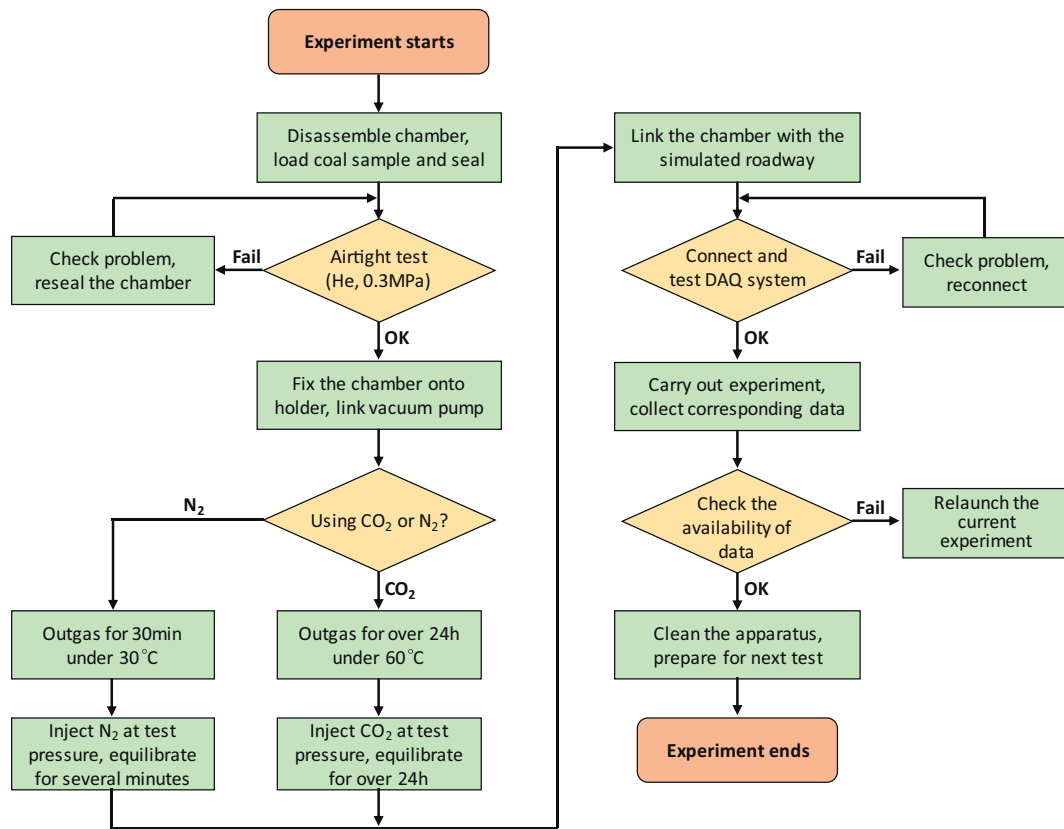


Fig. 3. Flowchart of the outburst coal-gas flow experiment.

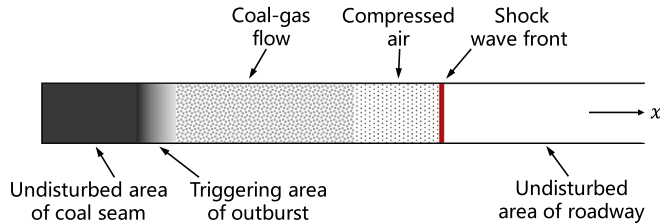


Fig. 4. Structural model of the outburst coal-gas flow.

strength depends on the outburst intensity (Cao et al. 2018; Zhou et al. 2015). Following the compressed air, is the coal-gas flow ejected from the triggering area of outburst and transporting in the status as fluidized flow (Kissell and Iannacchione 2014; Xu et al. 2006). By fully analyzing the high-speed camera videos, the flow patterns of coal-gas two phase flow, which defined as the existing forms of the gas and solid phases (Cong et al. 2011; Kawahara et al. 2002; Kolev and Kolev 2005), were found to be highly chaos and changing frequently during its transport process. Referring to the pneumatic transport engineering, the flow patterns of a gas-solid two-phase flow can be classified as: suspension flow, dune flow, stratified flow and slug flow (Zhao et al. 2017), and in our experiment all of these four flow patterns were observed (see Fig. 5).

Generally, at the front portion of the coal-gas flow, the flow pattern appeared as the suspension flow composed of fine coal powder, which was caused by the combination of fine powder's excellent motion ability and the high-speed gas flow. Behind that, in the main body of coal-gas flow, the flow patterns were significantly affected by the factors such as outburst pressure, sample's particle size distribution (PSD) and the ejection distance. As shown in Fig. 5, under the conditions that the experimental sample was abundant in 1-3 mm coal particles or the outburst pressure was lower, the flow patterns of coal-gas flow would

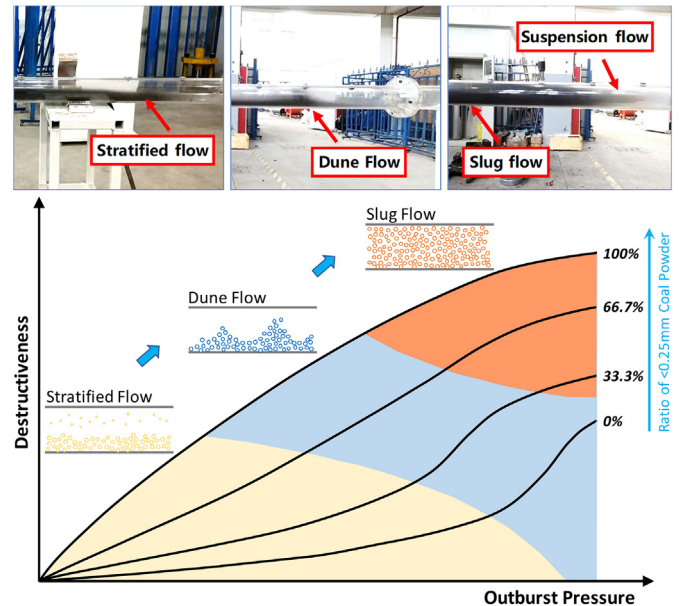


Fig. 5. Schematic diagram showing the influence factors of the outburst coal-gas flow.

be more likely to present the properties with obvious separation of gas/solid phases (like dune flow or stratified flow), and the destructiveness of the coal-gas flow would also be less serious (appearing as the smaller amount of ejected coal and shorter ejection distance). While under the conditions that the experimental sample was abundant in coal powder or the outburst pressure was higher, then the flow patterns were more likely to present the characteristics of fluidized status (like slug flow), and the destructiveness of the coal-gas flow would also be more serious

**Table 3**  
Experimental settings and the results of outburst coal-gas(CO<sub>2</sub>) flow tests.

Outburst pressure (MPa)	Sample #1		Sample #2		Sample #3		Sample #4	
	Loaded coal (kg)	Ejected coal (kg)						
0.1	8.668	1.762	10.983	4.646	10.696	5.395	9.489	6.271
0.3	8.668	3.017	10.975	6.278	10.711	6.915	9.475	7.312
0.5	8.644	4.112	10.984	7.080	10.576	7.753	9.846	8.383

(appearing as the larger amount of ejected coal and longer ejection distance). It should be noted that the dune flow and slug flow only occurred at the initial stage of transport, with the increase of ejection distance as well as the energy attenuation, nearly all of the flow patterns would be converted into stratified flow at the final transport stage, which mainly due to the weaker conveying capability of the low speed gas flow.

### 3.2. Intensity of outburst

To quantitatively evaluate the destructiveness of an outburst disaster, the intensity index of outburst which defined as the ejection amount of outburst coal are widely adopted. However, because of the density difference between coal particles/coal powder and the bulk density variation induced by granule arrangement (Rhodes 2008), the mass of coal loaded in the outburst chamber varied a lot for every test (see Table 3). Therefore, it is inappropriate to evaluate the intensities of experiments by directly comparing the mass of ejected coal.

To accurately evaluate the influence of outburst pressure and coal powder on outburst ejection, an index of relative intensity of outburst (RIO) was proposed to assess the intensities of the experiments (Geng et al. 2017; Xu et al. 2018), which was defined as the ratio of the ejected coal mass vs. the total loaded coal mass:

$$RIO = \frac{M_E}{M_L} \tag{1}$$

where RIO is the relative intensity of outburst, %;  $M_E$  is the mass of ejected coal after experiment, kg;  $M_L$  is the mass of coal loaded in the outburst chamber, kg.

Referring to Eq. (1), the experimental data was processed and the results (Table 4) indicated that the RIO values of experiments showed linear increasing tendency with the increasing of outburst pressure (see Fig. 6), and the maximum RIO reached 85.14%. For the tests under the same outburst pressure, the RIOs of CO<sub>2</sub> tests were 4.51–9.42% higher than that of N<sub>2</sub> tests, while the ejection distances of CO<sub>2</sub> tests were 0.49–2.12 m longer than that of N<sub>2</sub> tests (since for many cases, the ejected coal flow finally rushed out of the open end of simulated

**Table 4**  
RIO values and ejection distances of outburst coal-gas flow tests.

Sample ID	Outburst pressure (MPa)	RIO (%)		Ejection distance of coal (m)	
		CO <sub>2</sub> tests	N <sub>2</sub> tests	CO <sub>2</sub> tests	N <sub>2</sub> tests
Sample #1	0.1	20.33	15.82	3.05	1.48
	0.3	34.81	29.40	9.00	7.90
	0.5	47.57	43.15	10.30	9.02
Sample #2	0.1	42.30	35.32	5.38	4.78
	0.3	57.20	52.25	9.86	9.34
	0.5	64.46	58.56	11.75*	11.20*
Sample #3	0.1	50.44	–	6.23	–
	0.3	64.56	–	10.05*	–
	0.5	73.31	–	12.69*	–
Sample #4	0.1	66.09	58.03	5.75	3.63
	0.3	77.17	70.00	10.56*	10.07
	0.5	85.14	76.35	> 13.65*	12.65*

\* Ejected coal rushed out of the open end of simulated roadway.

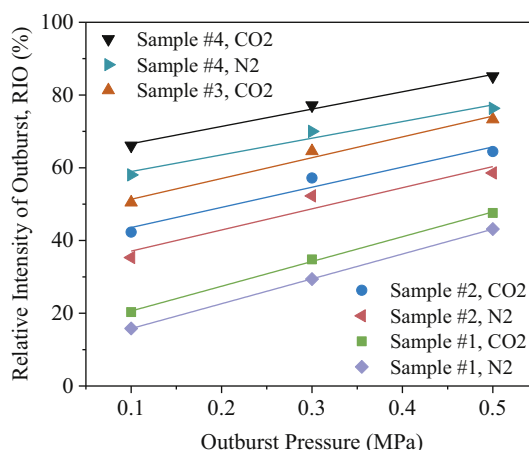


**Fig. 6.** Relationship between outburst pressure and the relative intensity of outburst (RIO).

roadway, thus the data of the ejection distance was not very accurate), which indicated that the gas desorption from coal can enhance the intensity and destructiveness of the outburst.

Besides, it was also found that with the increase of coal powder's ratio in the experimental samples, the differences of RIOs between CO<sub>2</sub> and N<sub>2</sub> tests became bigger and bigger (for sample #1 the average difference of RIO was 4.78%; for sample #2 the average difference was 5.94%; while for sample #4 the average difference reached 8.01%), which demonstrated that the outburst would be significantly intensified by the rapid gas desorption from the tectonic deformation induced powdered coal in the coal seam.

### 3.3. Transport features of outburst coal-gas flow

#### 3.3.1. Shockwave

To acquire the shockwave data of outburst coal-gas flow, three high frequency pressure transmitters (named as PT #1, PT #2 and PT #3 respectively) were set on the simulated roadway of apparatus to record the pressure variations during the experiment. And two other pressure transmitters (named as C#1 and C#2 respectively) were installed on the outburst chamber to calculate when the simulated outburst was triggered (defining the pressure-drop moment of pressure transmitter as the moment that the exposed coal surface reached the sensor's position, then by the data obtained from C#1 and C#2 the propagation speed of exposed surface in the outburst chamber could be acquired. Because this propagation speed was generally presumed as constant and the spacing between C#1 and the outburst mouth was already known, thus the triggering moment could be calculated). The arrangement of pressure transmitters on the apparatus is shown in Fig. 7. The logging frequency of the transmitters are all set to be 2000 Hz, namely recording a data every 0.5 ms.

Previous studies used to simplified the development stage of outburst as a uniformity jet flow of high pressure gas, and therefore deduced that the propagation of outburst shockwave in the roadway should obey the equation as Eq. (2) (Wang et al. 2011), which indicate that the propagation law of shockwave has two features: 1) the strength

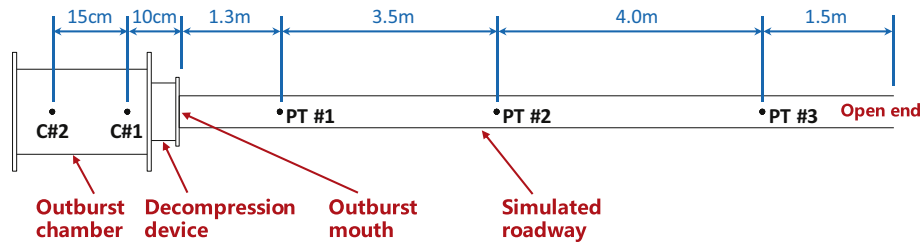


Fig. 7. Schematic diagram showing the arrangement of high frequency pressure transmitters.

of shockwave overpressure is proportional to the outburst energy, and inversely proportional to the propagation distance as well as the cross-sectional area of the roadway; 2) with the increase of propagation distance, the decay rate of overpressure will get faster and faster.

$$\Delta P = \frac{2(k + 1)^2(k - 1)}{3k - 1} \cdot \frac{W}{s} \cdot \frac{1}{x} \quad (2)$$

where  $\Delta P$  is the overpressure (belong to static pressure) of the shockwave, MPa;  $k$  is the gas compressibility factor;  $W$  is the work that gas expansion done on air medium, J;  $s$  is the cross-sectional area of the underground roadway,  $m^2$ ;  $x$  is the distance that shockwave propagates in the roadway, m.

Eq. (2) seems to be correct when we checked it with the data from controlled experiments using  $N_2$  (see Table 5 and Fig. 8a), the propagation regularity of shockwave overpressure obeyed these two features well. However, for the  $CO_2$  tests, the results varied significantly as shown in Fig. 8b. With the influence from gas desorption, especially under the condition that the powdered coal ratio and outburst pressure were high, the following characteristics were noticed: 1) for the experimental samples that were abundant in 1-3 mm coal particles, the differences between  $CO_2$  and  $N_2$  tests were not remarkable; 2) for the experimental samples that were abundant in < 0.25 mm coal powder, when the outburst pressure was low the differences between  $CO_2$  and  $N_2$  tests were not remarkable as well, which may be attributed to the slow gas desorption rate of coal powder under low pressure. But with the increase of outburst pressure as well as the increase of the initial gas desorption rate of coal powder, the differences became more and more noticeable. For the tests using Sample #4, it could be found that under the gas pressure of 0.1 MPa ( $CO_2$  and  $N_2$ ), the peak values of shockwave overpressure monitored at different positions were highly similar. While under the gas pressure of 0.3 and 0.5 MPa, besides the distinctions at PT #2 positions, the peak overpressures obtained from PT #1 and PT #3 positions also showed remarkable differences (generally, the peak values of  $CO_2$  tests were 13.67%–63.22% larger than that of  $N_2$

tests). It should also be noted that due to the limitation of measurement range, the highest overpressure which transmitter can record was only 150 kPa, thus the real value of overpressure at PT #2 position may be even higher.

Moreover, from the overpressure waveforms recorded by the pressure transmitters, it was found that the above 150 kPa overpressure appeared at PT #2 position when using  $CO_2$  to conduct the experiments (see Fig. 9b and c) last for a certain duration rather than just in one moment as shown in Fig. 9a and d, but similar phenomenon was not observed in the controlled experiments using  $N_2$  (see Fig. 9e and f). The duration of high static overpressures not only indicated that the destructiveness (e.g. shockwave overpressure) of outburst coal-gas flow could be significantly intensified by the rapid gas desorption from powdered coal, but also demonstrated that the transport type of coal-gas flow was changed from the dynamic pressure pneumatic conveying to the static pressure conveying, which mean that the outburst coal-gas flow influenced by rapid gas desorption would have much higher capability for conveying outburst coal/rock materials (Jaworski and Dyakowski 2002; Rhodes 2008; Yang et al. 2011), rather than a simple ejection driven by the high pressure free gas in the chamber or outburst hole.

### 3.3.2. Motion speed of coal flow

To completely record the motion characteristics of outburst coal-gas flow in the simulated roadway, every pipe of the simulated roadway was monitored by a high-speed camera during the experiment. The motion speed of the ejected coal flow is calculated based on the imaging velocimetry method. Using the equal spacing arranged (25 cm) sensor connectors on every pipe as the reference objects, the key frames showing the moment when the coal flow's front passing through a particular position can be picked out by separating the high-speed video into frames, then the motion speed of the ejected coal flow can be calculated as:

Table 5  
Peak values of the shockwave overpressure induced by outburst coal-gas flow.

Sample ID	Distance from outburst mouth (m)	Peak value of shockwave overpressure (kPa)					
		$CO_2$ tests			$N_2$ tests		
		0.1 MPa	0.3 MPa	0.5 MPa	0.1 MPa	0.3 MPa	0.5 MPa
Sample #1	1.3	3.83	12.03	17.59	3.73	12.49	18.02
	4.8	3.07	8.22	13.01	3.57	8.30	16.09
	8.8	1.86	8.23	12.52	2.40	6.68	15.72
Sample #2	1.3	3.04	4.08	8.32	3.32	4.90	6.48
	4.8	2.38	4.25	6.68	2.51	4.87	5.01
	8.8	1.75	4.16	5.18	1.31	2.15	2.80
Sample #3	1.3	2.27	5.01	8.33	–	–	–
	4.8	2.31	6.48	151.89*	–	–	–
	8.8	1.19	2.80	6.18	–	–	–
Sample #4	1.3	2.58	7.90	13.03	2.60	6.95	10.55
	4.8	2.30	152.18*	152.19*	2.10	5.85	6.70
	8.8	1.44	5.68	7.47	1.52	3.48	5.13

\* Peak value data exceeded the measuring range of pressure transmitter (150 kPa).

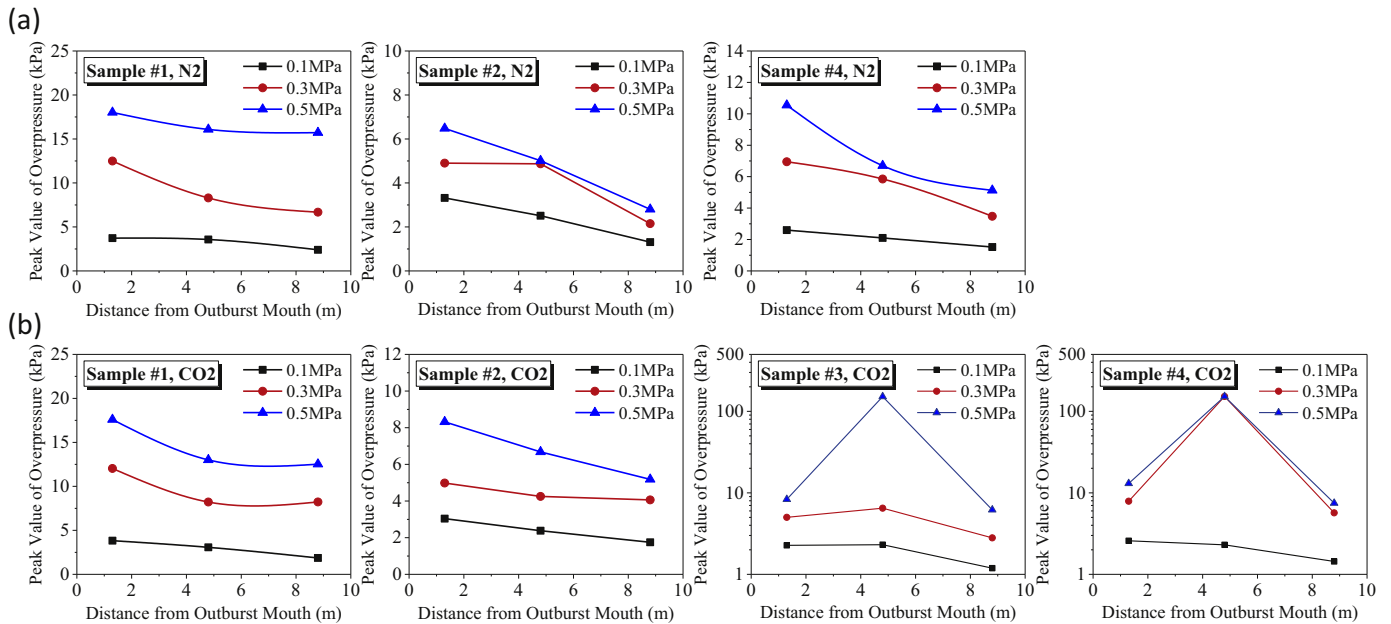


Fig. 8. Propagation characteristics of shockwave overpressure under different conditions of outburst pressure and experimental samples. (a) N<sub>2</sub> tests; (b) CO<sub>2</sub> tests.

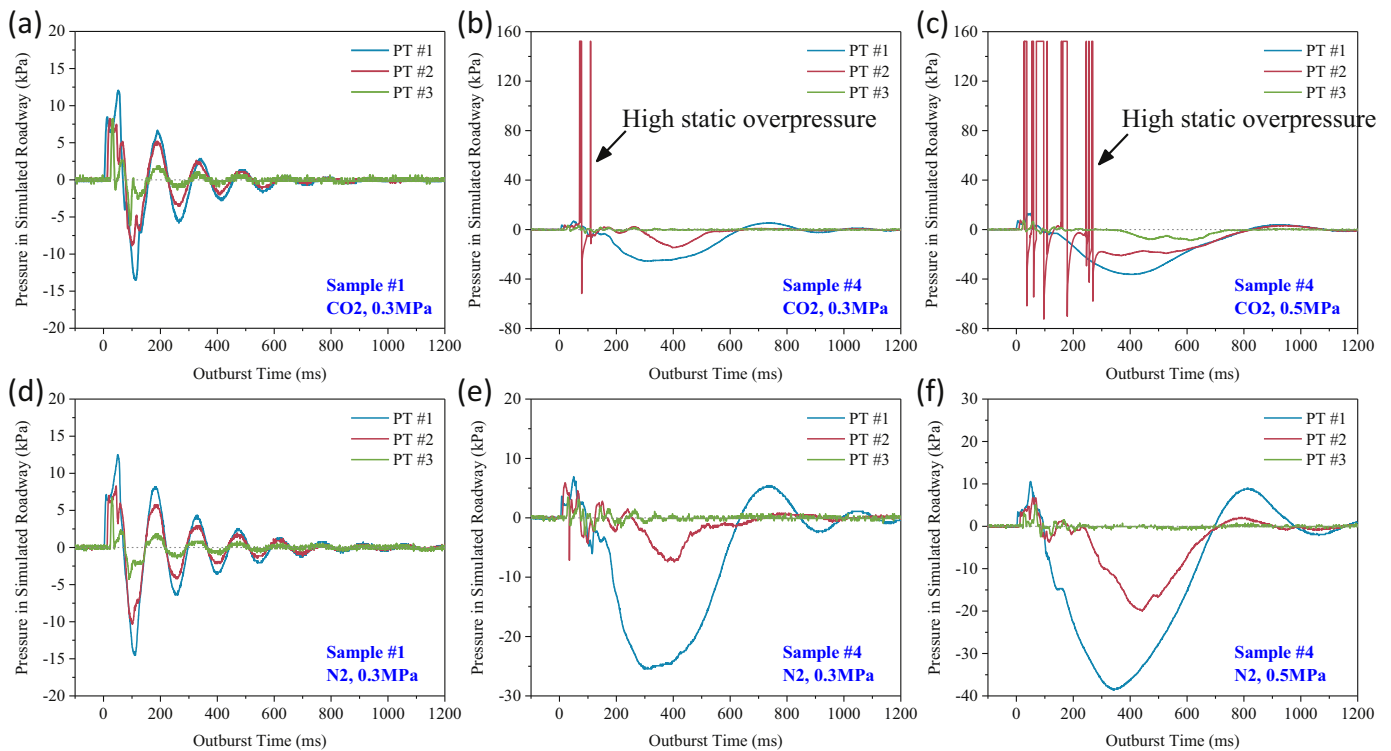


Fig. 9. Waveform comparisons of the shockwaves under different experimental conditions.

$$v_{cf} = \frac{\Delta L}{\Delta t} = \frac{\Delta L}{n \cdot \delta t} \quad (3)$$

where  $v_{cf}$  is the motion speed of the ejected coal flow, m/s;  $\Delta t$  is the time interval between two key frames, ms;  $\Delta L$  is the distance that coal flow's front passes through within  $\Delta t$ , m;  $n$  is number of frame interval between the two key frames;  $\delta t$  is the time interval for each frame, ms.

Using the imaging velocimetry method, the motion speed properties of the outburst coal-gas flow were obtained as Fig. 10. Once the outburst was triggered, the ejected coal would be accelerated by the drag force from high-speed gas flow. Due to the large gas pressure gradient

between the chamber and simulated roadway, the high-speed gas flow was of strong ability for carrying coal, thus the initial acceleration for the coal flow was very noticeable. From Fig. 10, it can be found that the velocity of coal flow was speed up from zero to 10–30 m/s just in < 2 m after the ejection, and the maximum coal flow speed measured from the experiments reached 41.02 m/s (sample #4 at 0.5 MPa CO<sub>2</sub>). After the initial acceleration, the drag force for coal flow decreased and gradually reached an equilibrium state with the air friction of the simulated roadway for most cases, resulting in a stable transport stage of the coal-gas flow. The duration of stable transport stage mainly depended on the

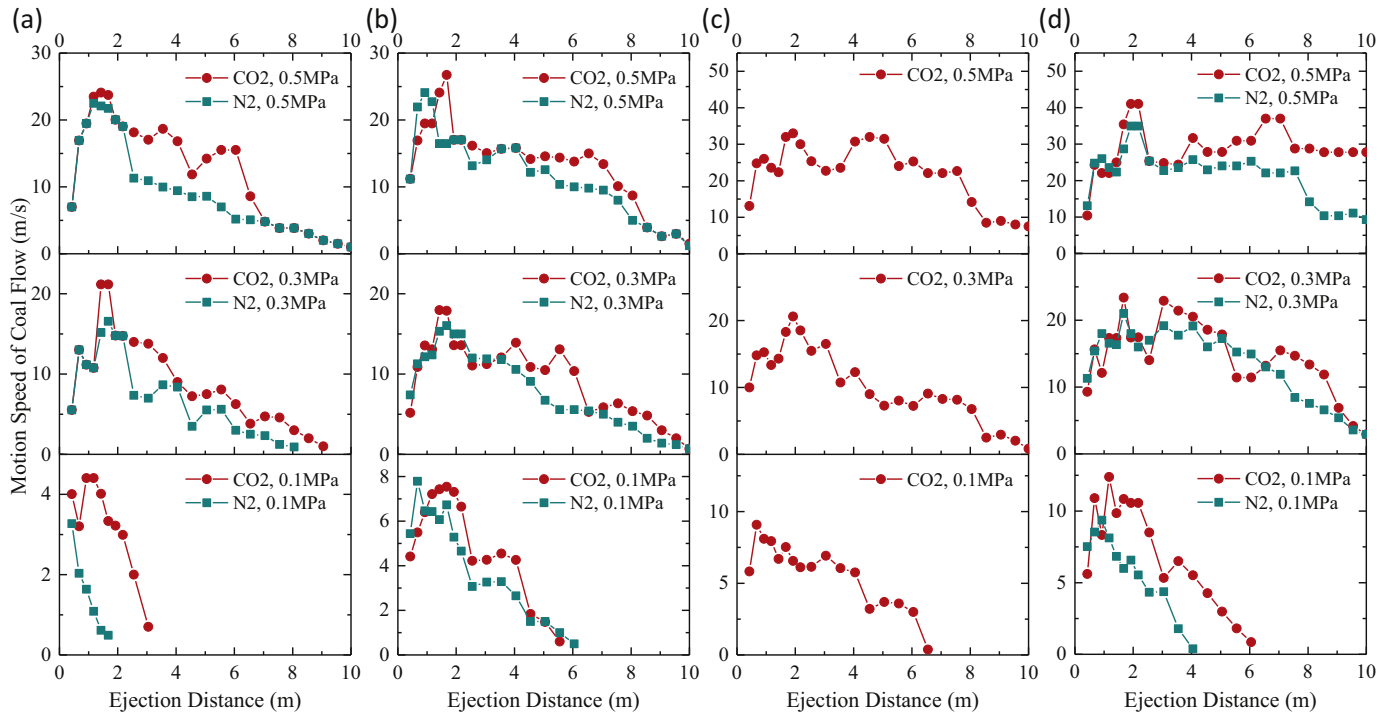


Fig. 10. Comparison of the coal flow's motion speed driven by different gases. (a) Sample #1; (b) Sample #2; (c) Sample #3; (d) Sample #4.

outburst pressure as well as the ingredient of experimental sample, it seemed that the stable transport situation of ejected coal was easier to be maintained with the condition of higher outburst pressure and high coal powder ratio. Moreover, under some conditions like high coal powder ratio and high CO<sub>2</sub> pressure, the coal flow could suffer a secondary acceleration during its transport process (see sample #3 at 0.5 MPa, sample #4 at 0.3 and 0.5 MPa), while similar phenomenon was never observed in the controlled tests even the outburst pressure was same, which proved that the impact of rapid gas desorption from powdered coal on the motion of coal flow did exist. After that, with the further increase of motion time and ejection distance, the speed of gas flow further decreased and its ability to carry outburst coal weakened as well, as a result, the separation phenomenon of coal/gas appeared and the motion speed of the ejected coal flow rapidly reduced until finally stopped, which indicated the termination of the outburst.

What should be noticed is, even though the majority of experimental phenomena showed that the motion process of ejected coal flow could be divided into three stages, namely the stages of acceleration, stable transport and decline (see Fig. 11a). But consider the impact induced by the tectonic deformation/pulverization of outburst-prone coal seam, we still believe that the Fig. 11b may better conform to the

reality of outburst coal flow transport underground, which demonstrated that the whole motion process of the outburst coal flow would go through the processes of initial acceleration, secondary acceleration, stable transport and decline.

In addition, when comparing the motion speed differences of coal flow between CO<sub>2</sub> tests and N<sub>2</sub> tests, it was further noticed that although their peak speeds (around the ejection distances of 1–2 m) were similar, however for the N<sub>2</sub> tests, either the duration of stable transport or the speed of stable transport were both smaller than that of CO<sub>2</sub> tests, even for the experimental samples that were abundant in 1–3 mm coal particles. This phenomenon further demonstrated that despite the rapid gas desorption from coal powder, the slower gas desorption from coal particles could also enhance the transport properties of outburst coal-gas flow. Since the diffusion coefficient of coal keeps constant when the size of coal particle exceeds 1 mm (Bertard et al. 1970; Bielicki et al. 1972), it can be concluded that during the actual outburst underground, the gas desorption from coal briquettes, coal particles and coal powder all have their effects on the promotion of outburst, but the majority of destructiveness is contributed by the rapid gas desorption from powdered coal.

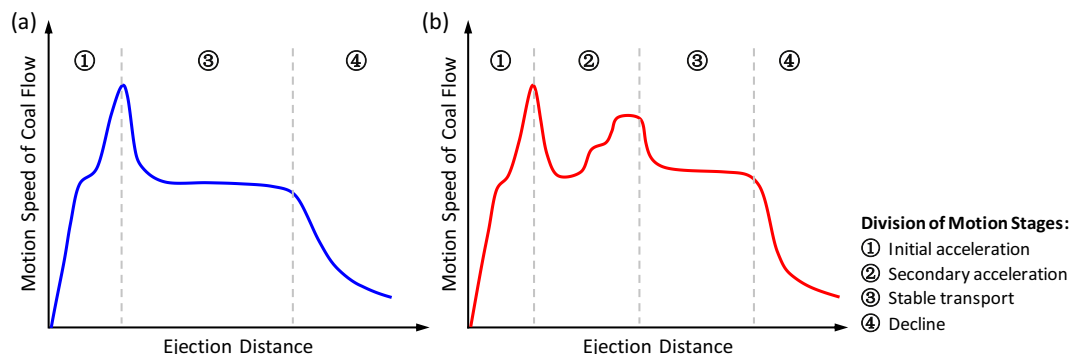


Fig. 11. Schematic diagram showing different motion patterns of the ejected coal flow in roadway.

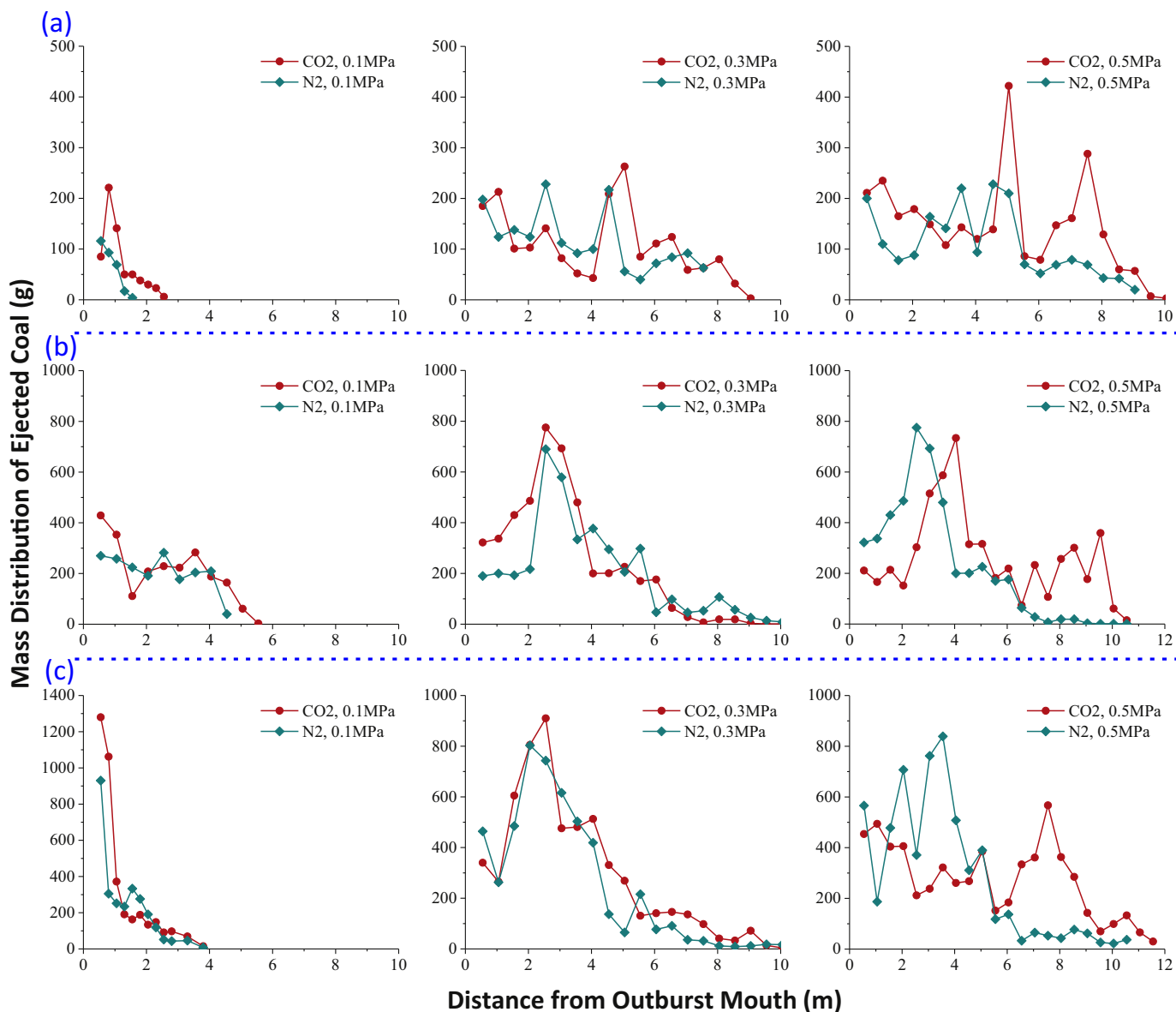


Fig. 12. Mass distributions of the deposited coal in the simulated roadway. (a) Sample #1; (b) Sample #2; (c) Sample #4.

### 3.4. Deposition characteristics of outburst coal

When the kinetic energy of outburst coal was exhausted, the ejected coals would deposit in the simulated roadway, appearing various deposition features. Through the statistics of the outburst coal's deposition characteristics, lots of information concerning the outburst could also be obtained.

#### 3.4.1. Mass distribution

After the experiment, the deposited coal in the simulated roadway would be carefully taken out by the interval of 50 cm using a long handle brush and weighed, the mass distribution characteristics of the deposited coal was shown in Fig. 12. Generally, with the increase of outburst pressure as well as the coal powder ratio, the mass of ejected coal deposition in the simulated roadway showed the trend of increment. And for the experiments under the low gas pressure of 0.1 MPa and 0.3MPa, due to the limited energy supply from slow gas desorption, the differences between CO<sub>2</sub> tests and N<sub>2</sub> tests were slight; the mass distribution curves of CO<sub>2</sub> tests were just slightly above the curves of N<sub>2</sub> tests. However, for the experiments under higher gas pressure, the

differences became much more obvious.

Moreover, from the Fig. 12 it can be noticed that in addition to the larger ejection amount, the mass distributions of CO<sub>2</sub> tests were much more likely to be concentrated in the front part of the simulated roadway when compared to that of N<sub>2</sub> tests, which indicated that the gas desorption from either coal particles or coal powder both have the influence on the transport of ejected coal, resulting in a longer ejection distance and high conveying capacity of the outburst coal as well as the more serious destructiveness.

#### 3.4.2. Pulverization

By sieving the ejected coal in the simulated roadway, the pulverization rate of the ejected coal (which was defined as the mass ratio of < 1 mm coal particle vs. the total mass of ejected coal) was obtained as Table 6. Results indicated that the pulverization properties of coal were closely related to the outburst pressure and the gas type. With the increase of outburst pressure, the pulverization rate showed increasing trend. However, when compared the CO<sub>2</sub> test results to the controlled experiments using N<sub>2</sub>, it was found that although the outburst pressure was same, the pulverization rate of CO<sub>2</sub> test was 2.66 times higher than

**Table 6**  
Pulverization characteristics of the ejected coal after experiments.

Outburst pressure (MPa)	Ejected coal amount (kg)	Coal amount of 1–3 mm (kg)	Coal amount of < 1 mm (kg)	Ratio of pulverization (%)
0.1 (CO <sub>2</sub> )	1.762	1.715	0.047	2.67
0.3 (CO <sub>2</sub> )	3.017	2.798	0.219	7.26
0.5 (CO <sub>2</sub> )	4.112	3.777	0.335	8.15
0.5 (N <sub>2</sub> )	3.369	3.248	0.121	3.06

that of N<sub>2</sub> test, which demonstrated that the gas ad-desorption of coal had significant influence on the pulverization of the coal during outburst. And the causes for this phenomenon may be attributed to the weakening of the coal induced by gas adsorption (Lin et al. 2017; Liu et al. 2011; Ranathunga et al. 2016; Wang et al. 2013c), or the so called “popcorn” cracking induced by free gas expansion in the pore/cleat system of the coal (Ubhayakar et al. 1977; Wang et al. 2015), or the collision pulverization of the high speed ejected coal particles (Teng et al. 2009; Zhang and Ghadiri 2002), which still need further studies.

Besides, the PSD analyses of the ejected coal demonstrated that in the CO<sub>2</sub> tests, coal suffered much more serious pulverization than that in the N<sub>2</sub> controlled tests. As shown in Fig. 13, the PSD of deposited coal after CO<sub>2</sub> outburst had a much wider range of distribution, while in the N<sub>2</sub> test the coal seemed hardly to be crushed into the particle size below 0.5–1 mm. The much more serious pulverization for the ejected coal during the development stage of outburst could enhance the gas desorption characteristics of the outburst coal during its transport process through the roadway, which would also promote the outburst coal-gas flow and enhance the destructiveness of the outburst.

## 4. Discussion

### 4.1. Energy principle in transport of outburst coal-gas flow

Through the experimental investigations concerning the formation and transport of outburst coal-gas flow, some special properties of the outburst coal-gas flow were revealed for the first time, such as the changes of transport types/flow patterns, enhanced shockwaves, self-accelerated coal flow, etc. However, due to the fact that there still exist many unknown factors hidden behind the outburst phenomena, to explain the outburst mechanism from a perspective of kinetics is full of difficulties, while explaining the outburst problem from the perspective of energy conservation seems to be a much more accessible way. For this, Hodot (1966) firstly proposed the energy principle for triggering outburst as:

$$W + Q > F + U \quad (4)$$

where  $W$  is the internal energy of gas in coal;  $Q$  is the elastic potential energy of coal;  $F$  is the energy consumption for outburst coal transport;  $U$  is the energy consumption for crushing coal.

With the development of research, the energy principle of outburst was further studied by a lot of scholars (Cai and Xiong 2005; Gray 1980; Jiang and Yu 1996; Valliappan and Wohua 1999; Zhao et al. 2016), their results (Eq. (3)) indicated that during the outburst, the outburst energy (including the gas expansion energy and the elastic energy of coal) was consumed in the transport and crushing of coal as well as the residual kinetic energy of gas flow after the separation of gas/solid phases.

$$W_1 + W_2 = A_1 + A_2 + A_3 \quad (5)$$

where  $W_1$  is the gas expansion energy in coal;  $W_2$  is the elastic energy of coal;  $A_1$  is energy consumption for the transport of outburst coal;  $A_2$  is the residual kinetic energy of the outburst gas flow;  $A_3$  is energy consumption for crushing coal.

However, as mentioned in the Introduction, the energy consumption for the ejection/transport of the outburst coal is mainly provided by the gas energy (Peng et al. 2012; Valliappan and Wohua 1999); while corresponding study also indicated that the elastic energy only account for a few thousandths of the total outburst energy (Zhao et al. 2016). Therefore, for the study of coal-gas flow transport in the development stage of outburst, the elastic energy of coal ( $W_2$ ) can be somehow ignored. Additionally, considering the low pulverization ratio of the experimental samples after the experiments, the energy consumption for crushing coal ( $A_3$ ) can be ignored as well. Thus, Eq. (3) can be simplified as:

$$W_1 = A_1 + A_2 \quad (6)$$

Since the outburst process is usually regarded as an adiabatic process occurring over a very short period (Chen 2011; Zhao et al. 2017), the gas expansion energy ( $W_1$ ) can be expressed as:

$$W_1 = \frac{p_0 V_0}{n-1} \left[ \left( \frac{p_1}{p_0} \right)^{\frac{n-1}{n}} - 1 \right] \quad (7)$$

where  $p_0$  is the atmospheric pressure in the roadway, usually  $p_0 = 0.1$  MPa;  $p_1$  is the outburst gas pressure (absolute pressure), MPa;  $V_0$  is the volume of gas that participated in the outburst, m<sup>3</sup>;  $n$  is the adiabatic coefficient, usually  $n = 1.31$ .

Also, because the outburst that the new apparatus simulates is a horizontal ejection of the coal-gas flow, the energy consumption for transporting outburst coal ( $A_1$ ) can be calculated using the formula of horizontal projectile motion as:

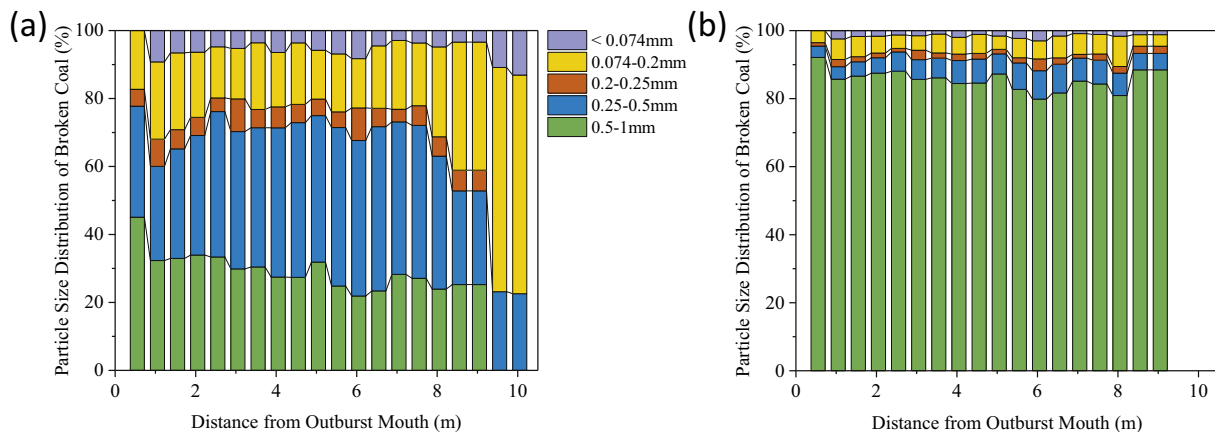


**Fig. 13.** Comparison of the pulverized coal's PSDs under different experimental gases. (a) Sample #1, 0.5 MPa, CO<sub>2</sub>; (b) Sample #1, 0.5 MPa, N<sub>2</sub>.

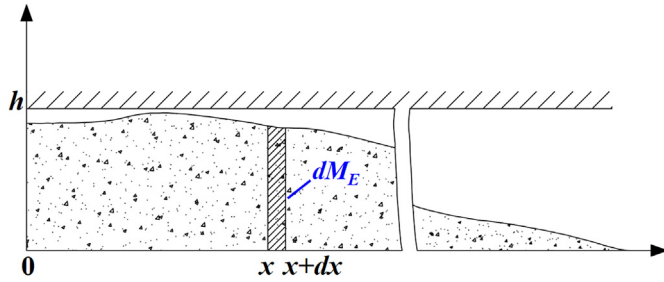


Fig. 14. Schematic diagram showing the deposition characteristic of outburst coal in roadway.

$$A_1 = \frac{1}{2}M_E v_e^2 = \frac{1}{2}M_E \cdot \left( \frac{L_e}{\sqrt{2 \cdot 0.5h/g}} \right)^2 = \frac{M_E \cdot L_e^2 \cdot g}{2h} \quad (8)$$

where  $L_e$  is the equivalent distance of coal ejection, m;  $g$  is the gravitational acceleration,  $g=9.8 \text{ m/s}^2$ ;  $h$  is the characteristic height dimension of the simulated roadway,  $h=0.1 \text{ m}$ .

The equivalent distance of coal ejection ( $L_e$ ) can be calculated from the deposition properties of the ejected coal (mass distribution) in the simulated roadway. As shown in Fig. 14, define an infinitesimal width of the ejected coal as  $dx$ , and the mass of the infinitesimal coal as  $dM$ , then the  $L_e$  of the ejection can be obtained as:

$$L_e = \frac{1}{M_E} \int x dM_E = \frac{1}{M_E} \sum_{i=1}^n (x_i \cdot dM_E) \quad (9)$$

The residual kinetic energy of the outburst gas flow ( $A_2$ ) can be theoretically calculated as below:

$$A_2 = \frac{1}{2}Q\rho_a v_a^2 \quad (10)$$

where  $Q$  is the volume of the outburst gas flow,  $\text{m}^3$ ;  $\rho_a$  is the density of the gas flow after the separation of gas and solid phases,  $\text{kg/m}^3$ ;  $v_a$  is the velocity of the outburst gas flow after the separation of gas and solid phases,  $\text{m/s}$ .

Due to the fact that the parameters in Eq. (8) are hardly to be acquired through experiments, the residual kinetic energy of the outburst gas flow is nearly impossible to be directly calculated. However, since the other two parameters ( $W_1$  and  $A_1$ ) in Eq. (4) are easily to be obtained, then  $A_2$  could be calculated as:  $A_2 = W_1 - A_1$ .

If we assume that the gas expansion energy ( $W_1$ ) was totally from the free gas in the outburst chamber, then based on the analyses of the energy principle in transport of outburst coal-gas flow (Eq. (4) to Eq. (7)), the basic parameters of the experimental samples (Table 2) and the experimental data, the energy characteristics of the development stage of outburst was able to be calculated as Table 7. From the table, it could be found that due to the similarity of the loaded coal's mass in the outburst chamber, the free gas expansion energy ( $W_1$ ) of the  $\text{CO}_2$  and

Table 7  
Energy characteristics of the development stage of outburst.

Sample ID	Outburst pressure (MPa)	Mass of loaded coal (kg)		Free gas expansion energy, $W_1$ (J)		Energy consumption for outburst coal transport, $A_1$ (J)		Residual kinetic energy of outburst gas flow, $A_2$ (J)	
		$\text{CO}_2$ tests	$\text{N}_2$ tests	$\text{CO}_2$ tests	$\text{N}_2$ tests	$\text{CO}_2$ tests	$\text{N}_2$ tests	$\text{CO}_2$ tests	$\text{N}_2$ tests
Sample #1	0.1	8.668	8.831	253.45	247.51	35.23	31.93	–	215.58
	0.3	8.668	8.644	1656.25	1661.97	868.72	784.54	–	877.43
	0.5	8.644	8.837	3767.34	3666.36	2300.46	1861.96	–	1804.40
Sample #2	0.1	10.983	10.944	181.28	182.66	460.93	145.06	–	37.6
	0.3	10.975	11.002	1186.48	1180.24	1896.13	804.06	–	376.18
	0.5	10.984	10.711	2684.78	2827.69	5792.01	1909.94	–	917.75
Sample #4	0.1	9.489	9.543	253.45	251.65	490.10	203.87	–	47.78
	0.3	9.475	9.599	1659.29	1632.31	2969.68	1434.39	–	197.92
	0.5	9.846	9.939	3578.28	3532.41	9336.26	2906.61	–	625.8

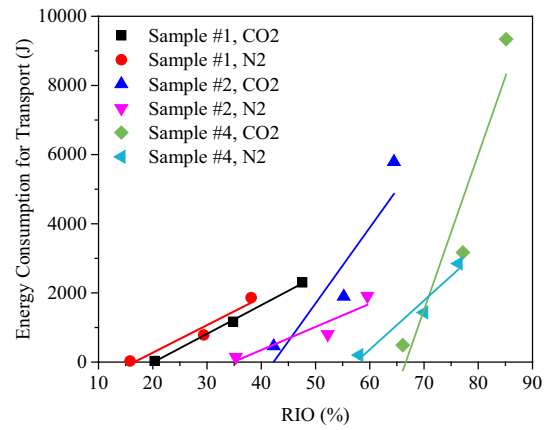


Fig. 15. Correlation between the relative intensity of outburst (RIO) and the energy consumption for coal transport.

$\text{N}_2$  tests were highly identical. Nevertheless, the calculation results for outburst coal transport ( $A_1$ ) indicated that the energy consumption of  $\text{CO}_2$  tests were much larger than that of  $\text{N}_2$  tests (the increase amplitude ranges from 10.34% to 221.21%). Moreover, with the increase of coal powder ratio as well as the outburst pressure, the growth proportion would get bigger and bigger (as shown in Fig. 15).

Besides, comparing the experimental data of Sample #2 and Sample #4 in Table 7, it could also be noticed that the values of  $A_1$  for  $\text{CO}_2$  tests were larger than their corresponding  $W_1$  while similar phenomenon were not found in  $\text{N}_2$  tests, which indicated that except for the free gas expansion, there existed other energy source for the  $\text{CO}_2$  tests. Since the whole apparatus was designed to be shut off from any other energy supplement during the experiments, such results proved that the gas desorption from the outburst coal would have significant effects on the promotion and ejection of the outburst coal, which would lead to much more serious catastrophic results of the outburst disaster. Meanwhile, to comprehensively express the energy principle of the gas expansion energy during the development stage of outburst, Eq. (5) should also be modified as Eq. (9):

$$W_1 = W_1^f + W_1^d = \frac{P_0}{n-1} (V_0^f + V_0^d) \left[ \left( \frac{P_1}{P_0} \right)^{\frac{n-1}{n}} - 1 \right] \quad (11)$$

where  $W_1^f$ ,  $W_1^d$  are the outburst energy provided by the free gas and adsorbed gas, respectively;  $V_0^f$ ,  $V_0^d$  are the volumes of the free gas and adsorbed gas that participated in the outburst, respectively.

#### 4.2. Effect of gas desorption on outburst

As shown in Table 7, because of the complex relation between  $W_1$  and  $A_1$  in  $\text{CO}_2$  tests, the corresponding residual kinetic energy of

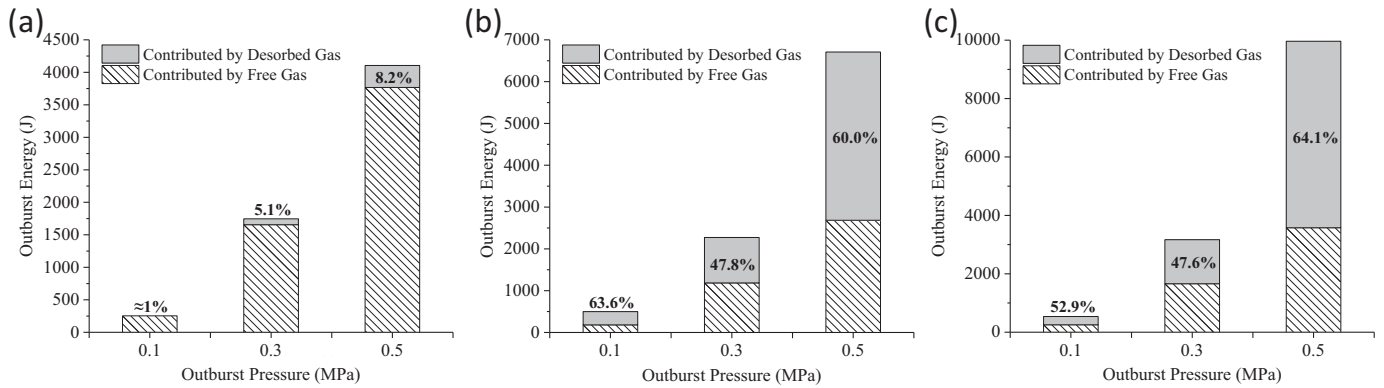


Fig. 16. Energy contributions of free and desorbed gas to the outburst coal transport. (a) Sample #1; (b) Sample #2; (c) Sample #4.

outburst gas flow ( $A_2$ ) was failed to be obtained. But for the  $N_2$  tests, the values of  $A_2$  were able to be calculated through the relationship of  $A_2 = W_1 - A_1$ . Thus, due to the similar separation gas speed for a certain particle-sized sample, it is reasonable to assume that the  $CO_2$  tests have the same values of  $A_2$  with the  $N_2$  tests, then the total outburst energy ( $W_1$ ) and the contribution ratio of gas desorption to the total energy ( $W_1^d/W_1$ ) can be calculated as Fig. 16.

With the increase of outburst pressure, the total outburst energy showed the trend of near-linear growth, and the contribution of desorbed gas in the total outburst energy also increase with the pressure (the maximum ratio of which reached 64.1%). In addition, comparing Fig. 16a with Fig. 16b and Fig. 16c, it can be found that when the outburst coal sample was composed by 100% of 1–3 mm coal particles, the effect of gas desorption on the transport of outburst coal was limited (the maximum contribution to the total energy was just 8.2%). However, when there exists a certain ratio of coal powder in the outburst coal sample, not only the total outburst energy suffered a great promotion (1.30–2.43 times), but also the contribution ratio of the desorbed gas exhibited an impressive step up (the average contribution ratio reached 56.0%). It meant that over half of the outburst energy were supplied by the gas desorption, almost equal to the additional energy increment when compared to the results of Fig. 16a, and of which the majority of the desorbed gas was provided by the rapid gas desorption from coal powder.

What should also be noted is that due to the large void volume induced by the natural stacking, the gas expansion energy produced by the free gas in the outburst chamber would be larger than that in a real underground outburst-prone coal seam (where the porosity would be smaller) under similar situation, thus for a real outburst disaster, the contribution ratio of rapid gas desorption would be much higher. Therefore, it could be concluded that the effect of the rapid gas desorption from powdered coal played a decisive role on the promotion of outburst.

## 5. Conclusions

1) In this paper, a new apparatus was used to study the formation, transport mechanism of outburst coal-gas flow. Experimental results indicated that during the development stage of outburst, the conveying pattern of outburst coal-gas flow in roadway belonged to the extremely complicated gas-solid two phase flow. The flow or destructiveness characteristics of outburst coal-gas flow were significantly affected by a number of factors, like outburst pressure, tectonic deformation (PSDs of the experimental samples), ejection distance, etc. With the increase of outburst pressure, the relative intensity of outburst (RIO index) and the total outburst energy both exhibited the variation trend of near-linear growth, as well as the pulverization characteristics of ejected coal. Besides, with the increase of the coal powder ratio in the experimental sample, the RIO

values and the total outburst energy of the simulated outburst were also significantly enhanced, which demonstrated that the powdered coal played an important role in the promotion of underground outburst disasters.

- 2) By comparing the results of outburst coal-gas flow experiments (using  $CO_2$ ) and the controlled experiments (using  $N_2$ , to rule out the influence from gas ad-desorption), it was revealed that influenced by the gas desorption of coal, the destructiveness and transport features of outburst coal-gas flow could be significantly affected. Generally, with the effect of gas desorption ( $CO_2$  tests), the total outburst energy was promoted by 1.30–2.43 times; the peak values of outburst shockwave were enhanced by at least 13.67%–63.22%; the transport type of coal-gas flow was changed from dynamic pressure pneumatic conveying to the static pressure conveying which could provide higher capability for conveying outburst coal/rock materials; the motion of the ejected coal flow could suffer secondary acceleration under certain situations, thus longer duration of stable transport as well as higher transport speed could be provided. Additionally, with the influence of gas desorption, the ejected coal was much more likely to be deposited in the front part of the simulated roadway and suffered more serious pulverization (the pulverization rate of  $CO_2$  test was 2.66 times higher than that of  $N_2$  test), which would enhance the destructiveness of the outburst. Furthermore, all of the above-mentioned influences were sensitive to the PSDs of the experimental samples, namely sensitive to the different initial gas desorption properties of different sized coal. For this, experiments further indicated that the coal particles and coal powder both had impacts on the transport of outburst coal-gas flow, however because the  $< 0.25$  mm coal powder in the experimental sample had more rapid initial gas desorption rate, its effect on the transport and deposit characteristics of outburst coal-gas flow was much more remarkable.
- 3) The energy analyses on the transport of outburst coal-gas flow indicated that the total outburst energy was mainly consumed in the conveying of the ejected coal; what's more, the energy supplied by free gas expansion was insufficient for the transport process, whilst the difference was made up by the energy from gas desorption. Based on the principle of energy conservation, the effect of gas desorption on the outburst development was evaluated and the result demonstrated that over half of the outburst energy (average contribution ratio reached 56.0% while the maximum reached 64.1%) could be supplied by the gas desorption, and of which the majority of desorbed gas was provided by the rapid gas desorption from powdered coal. When spreading this laboratory result to the in-site conditions (where the porosity of the coal seam was smaller), the contribution of gas desorption would be much greater. Thus, it could be concluded that the effect of the rapid gas desorption from powdered coal played a decisive role on the promotion of outburst.

## Acknowledgements

The authors are grateful to the financial support from the Fundamental Research Funds for the Central Universities (2017XKZD01) and the Project Funded by the Priority Academic Program Development of Jiangsu Higher Education Institutions (PAPD).

## References

- Aguado, M.B.D., Nicieza, C.G., 2007. Control and prevention of gas outbursts in coal mines, Riosa–Olloniego coalfield, Spain. *Int. J. Coal Geol.* 69, 253–266.
- An, F., Cheng, Y., 2014. An explanation of large-scale coal and gas outbursts in underground coal mines: the effect of low-permeability zones on abnormally abundant gas. *Nat. Hazards Earth Syst. Sci.* 14, 2125–2132.
- An, F.-h., Cheng, Y.-p., Wang, L., Li, W., 2013. A numerical model for outburst including the effect of adsorbed gas on coal deformation and mechanical properties. *Comput. Geotech.* 54, 222–231.
- Beamish, B.B., Crosdale, P.J., 1998. Instantaneous outbursts in underground coal mines: an overview and association with coal type. *Int. J. Coal Geol.* 35, 27–55.
- Bertard, C., Bruyet, B., Gunther, J., 1970. Determination of desorbable gas concentration of coal (direct method). *Int. J. Rock Mech. Min. Sci. Geomech. Abstr.* 43–65 Elsevier.
- Bielicki, R.J., Perkins, J.H., Kissell, F.N., 1972. Methane Diffusion Parameters for Sized Coal Particles: A Measuring Apparatus and some Preliminary Results. Bureau of Mines, Washington, DC (USA).
- Briggs, H., 1921. Characteristics of outbursts of gas in mines. *Trans. Inst. Min. Eng.* 61, 119–146.
- Cai, C., Xiong, Y., 2005. Theoretical and experimental study on crushing energy of outburst-proneness coal. *J. China Coal Soc.* 30, 63–66.
- Cao, J., Sun, H., Dai, L., Sun, D., Wang, B., Miao, F., 2018. Simulation research on dynamic effect of coal and gas outburst. *J. China Univ. Min. Technol.* 47, 113–120.
- Chen, K.P., 2011. A new mechanistic model for prediction of instantaneous coal outbursts—dedicated to the memory of Prof. Daniel D. Joseph. *Int. J. Coal Geol.* 87, 72–79.
- Cong, X., Guo, X., Gong, X., Lu, H., Dong, W., 2011. Experimental research of flow patterns and pressure signals in horizontal dense phase pneumatic conveying of pulverized coal. *Powder Technol.* 208, 600–609.
- Cui, X., Bustin, R.M., Dipple, G., 2004. Selective transport of CO<sub>2</sub>, CH<sub>4</sub>, and N<sub>2</sub> in coals: insights from modeling of experimental gas adsorption data. *Fuel* 83, 293–303.
- Fan, C., Li, S., Luo, M., Du, W., Yang, Z., 2017. Coal and gas outburst dynamic system. *Int. J. Min. Sci. Technol.* 27, 49–55.
- Farmer, I., Pooley, F., 1967. A hypothesis to explain the occurrence of outbursts in coal, based on a study of West Wales outburst coal. *Int. J. Rock Mech. Min. Sci. Geomech. Abstr.* 189–193 Elsevier.
- Flores, R.M., 1998. Coalbed methane: from hazard to resource. *Int. J. Coal Geol.* 35, 3–26.
- Geng, J., Xu, J., Nie, W., Peng, S., Zhang, C., Luo, X., 2017. Regression analysis of major parameters affecting the intensity of coal and gas outbursts in laboratory. *Int. J. Min. Sci. Technol.* 27, 327–332.
- Gray, I., 1980. The Mechanism of, and Energy Release Associated with Outbursts, Symposia Series. Australasian Institute of Mining and Metallurgy, pp. 111–125.
- Hodot, B.B., 1966. Outburst of Coal and Coalbed Gas. China Industry Press, Beijing.
- Hu, Q., Wen, G., 2013. Coal and Gas Outburst Mechanical Mechanism. Science Press, Beijing.
- Jaworski, A.J., Dykowski, T., 2002. Investigations of flow instabilities within the dense pneumatic conveying system. *Powder Technol.* 125, 279–291.
- Jiang, C., Yu, Q., 1996. Rules of energy dissipation in coal and gas outburst [J]. *J. China Coal Soc.* 21, 173–178.
- Jiang, C., Xu, L., Li, X., Tang, J., Chen, Y., Tian, S., Liu, H., 2015. Identification model and indicator of outburst-prone coal seams. *Rock Mech. Rock. Eng.* 48, 409–415.
- Jin, K., Cheng, Y., Liu, Q., Zhao, W., Wang, L., Wang, F., Wu, D., 2016a. Experimental investigation of pore structure damage in pulverized coal: implications for methane adsorption and diffusion characteristics. *Energy Fuel* 30, 10383–10395.
- Jin, K., Cheng, Y., Wang, W., Liu, H., Liu, Z., Zhang, H., 2016b. Evaluation of the remote lower protective seam mining for coal mine gas control: a typical case study from the Zhuxianzhuang coal mine, Huaibei coalfield, China. *J. Nat. Gas Sci. Eng.* 33, 44–55.
- Karacan, C.Ö., Ruiz, F.A., Coté, M., Phipps, S., 2011. Coal mine methane: a review of capture and utilization practices with benefits to mining safety and to greenhouse gas reduction. *Int. J. Coal Geol.* 86, 121–156.
- Kawahara, A., Chung, P.-Y., Kawaji, M., 2002. Investigation of two-phase flow pattern, void fraction and pressure drop in a microchannel. *Int. J. Multiphase Flow* 28, 1411–1435.
- Kelemen, S., Kwiatek, L., 2009. Physical properties of selected block Argonne premium bituminous coal related to CO<sub>2</sub>, CH<sub>4</sub>, and N<sub>2</sub> adsorption. *Int. J. Coal Geol.* 77, 2–9.
- Kissell, F.N., Iannacchione, A.T., 2014. Gas outbursts in coal seams. In: *Coal Bed Methane: From Prospect to Pipeline*, pp. 177.
- Kolev, N.I., Kolev, N., 2005. *Multiphase Flow Dynamics*. Springer.
- Lama, R., Bodziony, J., 1998. Management of outburst in underground coal mines. *Int. J. Coal Geol.* 35, 83–115.
- Lin, J., Ren, T., Wang, G., Booth, P., Nemicik, J., 2017. Experimental study of the adsorption-induced coal matrix swelling and its impact on ECBM. *J. Earth Sci.* 28, 917–925.
- Lin, J., Ren, T., Wang, G., Booth, P., Nemicik, J., 2018. Experimental investigation of N<sub>2</sub> injection to enhance gas drainage in CO<sub>2</sub>-rich low permeable seam. *Fuel* 215, 665–674.
- Liu, J., Chen, Z., Elsworth, D., Qu, H., Chen, D., 2011. Interactions of multiple processes during CBM extraction: a critical review. *Int. J. Coal Geol.* 87, 175–189.
- Lu, C.-P., Dou, L.-M., Liu, H., Liu, H.-S., Liu, B., Du, B.-B., 2012. Case study on microseismic effect of coal and gas outburst process. *Int. J. Rock Mech. Min. Sci.* 53, 101–110.
- Lu, C.-P., Dou, L.-M., Zhang, N., Xue, J.-H., Liu, G.-J., 2014. Microseismic and acoustic emission effect on gas outburst hazard triggered by shock wave: a case study. *Nat. Hazards* 73, 1715–1731.
- Lu, S., Li, L., Cheng, Y., Sa, Z., Zhang, Y., Yang, N., 2017. Mechanical failure mechanisms and forms of normal and deformed coal combination containing gas: model development and analysis. *Eng. Fail. Anal.* 80, 241–252.
- Noack, K., 1998. Control of gas emissions in underground coal mines. *Int. J. Coal Geol.* 35, 57–82.
- Otuonye, F., Sheng, J., 1994. A numerical simulation of gas flow during coal/gas outbursts. *Geotech. Geol. Eng.* 12, 15–34.
- Paterson, L., 1986. A model for outbursts in coal. *Int. J. Rock Mech. Min. Sci. Geomech. Abstr.* 327–332 Elsevier.
- Peng, S., Xu, J., Yang, H., Liu, D., 2012. Experimental study on the influence mechanism of gas seepage on coal and gas outburst disaster. *Saf. Sci.* 50, 816–821.
- Ranathunga, A., Perera, M., Ranjith, P., 2016. Influence of CO<sub>2</sub> adsorption on the strength and elastic modulus of low rank Australian coal under confining pressure. *Int. J. Coal Geol.* 167, 148–156.
- Rhodes, M.J., 2008. *Introduction to Particle Technology*. John Wiley & Sons.
- Shepherd, J., Rixon, L., Griffiths, L., 1981. Outbursts and geological structures in coal mines: a review. *Int. J. Rock Mech. Min. Sci. Geomech. Abstr.* 267–283 Elsevier.
- Sun, D.-I., Miao, F.-t., Liang, Y.-p., 2009. Study on the formation mechanism of shock wave in process of coal and gas outburst. *Journal of Coal Science and Engineering (China)* 15, 134–137.
- Sun, D., Hu, Q., Miao, F., 2011. A mathematical model of coal-gas flow conveying in the process of coal and gas outburst and its application. *Proc. Eng.* 26, 147–153.
- Teng, S., Wang, P., Zhu, L., Young, M.-W., Gogos, C.G., 2009. Experimental and numerical analysis of a lab-scale fluid energy mill. *Powder Technol.* 195, 31–39.
- Tu, Q., Cheng, Y., Guo, P., Jiang, J., Wang, L., Zhang, R., 2016. Experimental study of coal and gas outbursts related to gas-enriched areas. *Rock Mech. Rock. Eng.* 49, 3769–3781.
- Tu, Q., Cheng, Y., Liu, Q., Guo, P., Wang, L., Zhao, W., Li, W., Dong, J., 2017. An analysis of the layered failure of coal: new insights into the flow process of outburst coal. *Environ. Eng. Geosci.* 23 (4), 1–13 (1078-7275. EEG-1963).
- Ubhayakar, S.K., Stickler, D.B., Von Rosenberg, C.W., Gannon, R.E., 1977. Rapid devolatilization of pulverized coal in hot combustion gases. *Symp. Combust.* 427–436 Elsevier.
- Valliappan, S., Wohua, Z., 1999. Role of gas energy during coal outbursts. *Int. J. Numer. Methods Eng.* 44, 875–895.
- Wang, K., Zhou, A.-t., Zhang, P., Li, C., Guo, Y.-w., 2011. Study on the propagation law of shock wave resulting from coal and gas outburst. *J. Coal Sci. Eng. (China)* 17, 142–146.
- Wang, K., Zhou, A., Zhang, J., Zhang, P., 2012. Real-time numerical simulations and experimental research for the propagation characteristics of shock waves and gas flow during coal and gas outburst. *Saf. Sci.* 50, 835–841.
- Wang, H., Cheng, Y., Yuan, L., 2013a. Gas outburst disasters and the mining technology of key protective seam in coal seam group in the Huainan coalfield. *Nat. Hazards* 67, 763–782.
- Wang, L., Cheng, Y.-P., Xu, C., An, F.-h., Jin, K., Zhang, X.-l., 2013b. The controlling effect of thick-hard igneous rock on pressure relief gas drainage and dynamic disasters in outburst coal seams. *Nat. Hazards* 66, 1221–1241.
- Wang, S., Elsworth, D., Liu, J., 2013c. Permeability evolution during progressive deformation of intact coal and implications for instability in underground coal seams. *Int. J. Rock Mech. Min. Sci.* 58, 34–45.
- Wang, S., Elsworth, D., Liu, J., 2015. Rapid decompression and desorption induced energetic failure in coal. *J. Rock Mech. Geotech. Eng.* 7, 345–350.
- Xu, L., Jiang, C., 2017. Initial desorption characterization of methane and carbon dioxide in coal and its influence on coal and gas outburst risk. *Fuel* 203, 700–706.
- Xu, T., Tang, C., Yang, T., Zhu, W., Liu, J., 2006. Numerical investigation of coal and gas outbursts in underground collieries. *Int. J. Rock Mech. Min. Sci.* 43, 905–919.
- Xu, J., Geng, J., Peng, S., Yuan, M., Zhang, C., Luo, X., 2018. Analysis of the pulsating development process of coal and gas outburst. *J. China Univ. Min. Technol.* 47, 145–154.
- Xue, S., Wang, Y., Xie, J., Wang, G., 2011. A coupled approach to simulate initiation of outbursts of coal and gas—model development. *Int. J. Coal Geol.* 86, 222–230.
- Xue, S., Yuan, L., Wang, J., Wang, Y., Xie, J., 2015. A coupled DEM and LBM model for simulation of outbursts of coal and gas. *Int. J. Coal Sci. Technol.* 2, 22–29.
- Yang, D., Zhou, B., Xu, C., Wang, S., 2011. Dense-phase pneumatic conveying under pressure in horizontal pipeline. *Particology* 9, 432–440.
- Ye, Q., Jia, Z., Zheng, C., 2017a. Study on hydraulic-controlled blasting technology for pressure relief and permeability improvement in a deep hole. *J. Pet. Sci. Eng.* 159, 433–442.
- Ye, Q., Wang, G.G.X., Jia, Z., Zheng, C., 2017b. Experimental study on the influence of wall heat effect on gas explosion and its propagation. *Appl. Therm. Eng.* 118, 392–397.
- Ye, Q., Wang, G., Jia, Z., Zheng, C., Wang, W., 2018. Similarity simulation of mining-crack-evolution characteristics of overburden strata in deep coal mining with large dip. *J. Pet. Sci. Eng.* 165, 477–487.
- Zhang, Z., Ghadiri, M., 2002. Impact attrition of particulate solids. Part 2: experimental work. *Chem. Eng. Sci.* 57, 3671–3686.
- Zhao, W., Cheng, Y., Yuan, M., An, F., 2014. Effect of adsorption contact time on coking

- coal particle desorption characteristics. *Energy Fuel* 28, 2287–2296.
- Zhao, W., Cheng, Y., Jiang, H., Jin, K., Wang, H., Wang, L., 2016. Role of the rapid gas desorption of coal powders in the development stage of outbursts. *Journal of Natural Gas Science and Engineering* 28, 491–501.
- Zhao, W., Cheng, Y., Guo, P., Jin, K., Tu, Q., Wang, H., 2017. An analysis of the gas-solid plug flow formation: new insights into the coal failure process during coal and gas outbursts. *Powder Technol.* 305, 39–47.
- Zhi, S., Elsworth, D., 2016. The role of gas desorption on gas outbursts in underground mining of coal. *Geomech. Geophys. Geo-Energ. Geo-Res.* 2, 151–171.
- Zhou, A., Wang, K., Wang, L., Du, F., Li, Z., 2015. Numerical simulation for propagation characteristics of shock wave and gas flow induced by outburst intensity. *Int. J. Min. Sci. Technol.* 25, 107–112.